2011

Ultrafast decay of hot phonons in an AlGaN/AlN/AlGaN/GaN camelback channel

J. H. Leach
Virginia Commonwealth University, s2jleach@vcu.edu

M. Wu
Virginia Commonwealth University

H. Morkoç
Virginia Commonwealth University, hmorkoc@vcu.edu

See next page for additional authors

Leach, J. H., Wu, M., & Morkoc, H., et al. Ultrafast decay of hot phonons in an AlGaN/AlN/AlGaN/GaN camelback channel. Journal of Applied Physics, 110, 104504 (2011).

Ultrafast decay of hot phonons in an AlGaN/AlN/AlGaN/GaN camelback channel

J. H. Leach,[1,a)] M. Wu,[1] H. Morkoç,[1] J. Liberis,[2] E. Šermukšnis,[2] M. Ramonas,[2] and A. Matulionis[2]
[1]*Virginia Commonwealth University, Richmond, Virginia 23284, USA*
[2]*Semiconductor Physics Institute of Center for Physical Science and Technology, Vilnius 01108, Lithuania*

(Received 17 May 2011; accepted 7 October 2011; published online 21 November 2011)

A bottleneck for heat dissipation from the channel of a GaN-based heterostructure field-effect transistor is treated in terms of the lifetime of nonequilibrium (hot) longitudinal optical phonons, which are responsible for additional scattering of electrons in the voltage-biased quasi-two-dimensional channel. The hot-phonon lifetime is measured for an $Al_{0.33}Ga_{0.67}N/AlN/Al_{0.1}Ga_{0.9}N/GaN$ heterostructure where the mobile electrons are spread in a composite $Al_{0.1}Ga_{0.9}N/GaN$ channel and form a camelback electron density profile at high electric fields. In accordance with plasmon-assisted hot-phonon decay, the parameter of importance for the lifetime is not the total charge in the channel (the electron sheet density) but rather the electron density profile. This is demonstrated by comparing two structures with equal sheet densities (1×10^{13} cm^{-2}), but with different density profiles. The camelback channel profile exhibits a shorter hot-phonon lifetime of ~270 fs as compared with ~500 fs reported for a standard $Al_{0.33}Ga_{0.67}N/AlN/GaN$ channel at low supplied power levels. When supplied power is sufficient to heat the electrons >600 K, ultrafast decay of hot phonons is observed in the case of the composite channel structure. In this case, the electron density profile spreads to form a camelback profile, and hot-phonon lifetime reduces to ~50 fs. © *2011 American Institute of Physics*. [doi:10.1063/1.3660264]

I. INTRODUCTION

GaN-based heterostructure field effect transistors (HFETs) are poised to dominate the high frequency-high power amplifier and switching markets.[1,2] In fact, AlGaN-based HFET structures are already available commercially for high power, moderate frequency applications. In the quest for increased cutoff frequencies, shorter gate lengths have been employed, but two-dimensional electron gas density (2DEG density) has also been observed to play a role in cutoff frequencies among devices from the same group.[3,4] For a given gate length, the cutoff frequencies tend to decrease with increasing 2DEG density. This can be explained in terms of the buildup of population of longitudinal optical (LO) phonons in the GaN channel.[5–7] The physical origin of the buildup is related to the fact that the time associated with the emission of LO phonons by hot electrons is much shorter than the time associated with the decay of these LO phonons into acoustic phonons. Consequently, the population builds-up, causes stronger electron scattering, and results in a decrease in electron drift velocity.[6,8] In addition to affecting the frequency performance of the HFET, the buildup is believed to be linked to the device reliability since the hot phonon population inevitably stimulates defect generation. Moreover, this can be envisaged when one considers that the hot phonons are crowded in a relatively narrow portion of the k-space where their equivalent temperature becomes extremely high.[9] In this regard, the generation of locally large atomic vibrations and ensuing new crystal defects is likely. Correlation of the hot-phonon lifetime and device degradation has been indirectly observed.[10]

The hot-phonon lifetime is a function of electron density, electron and ambient temperatures, and other conditions. In particular, time-resolved Raman studies in bulk GaN show that the hot-phonon lifetime decreases from about 2.5 to 0.35 ps as the carrier density increases from 10^{16} to 10^{19} cm^{-3}.[11] The monotonous decrease of the lifetime in bulk GaN is understood in terms of coupling of LO phonons with plasmons.[12]

Estimating the average three-dimensional electron density (3D density) in a HFET channel simply by dividing the sheet density by the effective width of the triangular quantum well at the Fermi energy we see that densities of the order of 10^{19} cm^{-3} and higher are readily attainable in the GaN channel of a HFET. As such, one might expect the hot-phonon lifetimes to be less than 0.35 ps in most 2DEGs. However, this often does not turn out to be the case. Experimental data on the hot-phonon lifetime in GaN 2DEGs at low applied fields obtained mainly through the microwave noise technique[13] are illustrated in Fig. 1 (open symbols) together with the experimental results for bulk GaN (closed circles) and those for the model of coupled plasmons and LO phonons (dashed line).

For an infinite electron plasma, the frequencies of uncoupled modes of plasmons and LO phonons would cross at the electron density,

$$n_{cr} = \omega_{LO}^2 \frac{m_e^* \varepsilon}{e^2}, \quad (1)$$

a)Author to whom correspondence should be addressed. Electronic mail: s2jleach@vcu.edu.

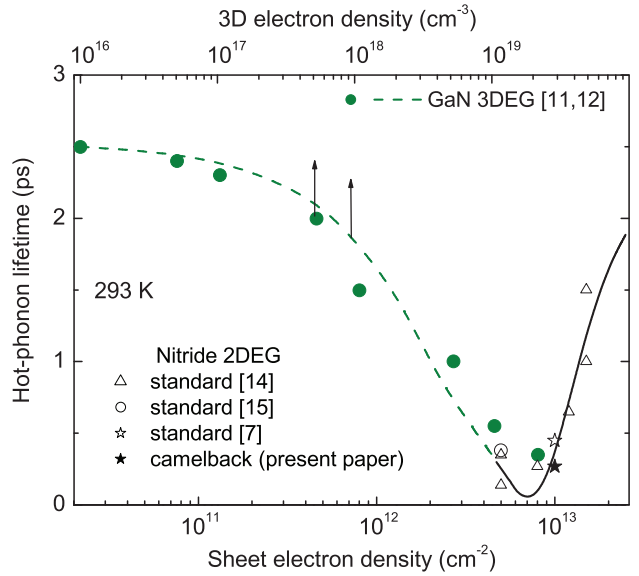

FIG. 1. (Color online) A survey of measured low field hot-phonon lifetimes for bulk GaN (closed circles, Ref. 11) and various GaN-based 2DEG channels (open symbols, Refs. 7, 14, 15) as well as the ($Al_{0.1}Ga_{0.9}N/GaN$) camelback channel (closed star) presented in this work. Dashed line stands for plasmon–LO-phonon model (Ref. 12). Solid line guides the eye. The resonance density is $\sim 7 \times 10^{12}$ cm^{-2}.

where ω_{LO} is the LO-phonon frequency at zero electron density and ε is the dielectric constant.[14] The coupled modes become most important at the crossover electron density, near 10^{19} cm^{-3} in bulk GaN. When the average 3D density in the channel is estimated as the 2DEG density divided by the width of the triangular well at the Fermi energy, the crossover is estimated to take place at $\sim 5 \times 10^{12}$ cm^{-2} in a typical GaN 2DEG channel.

The fastest decay of hot phonons is expected in the vicinity of the crossover. This expectation is in reasonable agreement with the non-monotonic resonance-type dependence of the hot-phonon lifetime on the 2DEG density measured at low fields for various nitride and arsenide heterostructure 2DEG channels.[14] The resonance for the nitride 2DEG channels is illustrated in Fig. 1 (open symbols and solid line).

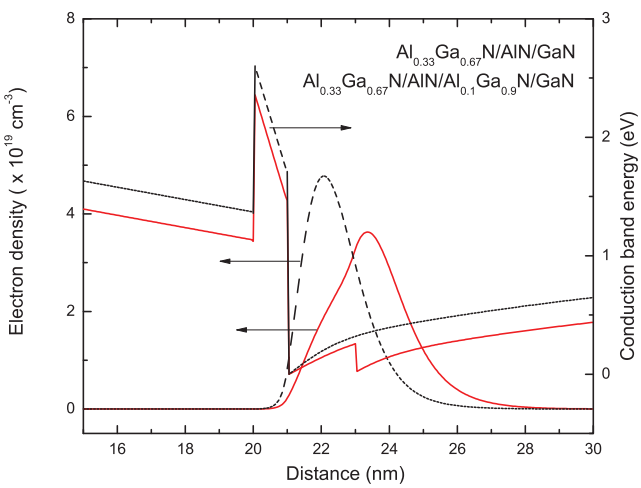

FIG. 2. (Color online) Calculated conduction band edge and electron 3D density for a standard (dashed lines) as well as the $Al_{0.1}Ga_{0.9}N$ camelback channel structure (solid lines). The total numbers of electrons are equal (1×10^{13} cm^{-2}) in each channel.

In light of the resonance phenomenon, the key to ultrafast decay of hot-phonons at high 2DEG densities (higher than the resonance 2DEG density estimated for standard 2DEG channels, Fig. 1) is in spreading the electrons in real space so that their 3D density can be made closer to the crossover density.[16] In this work, we illustrate this concept by presenting the measured hot-phonon lifetimes for two similar samples with almost identical 2DEG densities (1×10^{13} cm^{-2}) when a lower average bulk electron density is achieved in a composite $Al_{0.1}Ga_{0.9}N/GaN$ channel. The composite structure exhibits a "camelback" electron density profile under electron heating. The camelback profile is expected to have a bulk electron density closer to the resonance density needed to achieve the shortest hot-phonon lifetime.

II. SIMULATION

In order to estimate the effects of the camelback channel on the electron distribution in the 2DEG, Schrödinger–Poisson equations were solved for the structure in question as well as a standard HFET structure without the $Al_{0.1}Ga_{0.9}N$ interlayer. Results from the calculation are displayed in Fig. 2. One can observe two important points in the camelback device from Fig. 2. First, the conduction band edge changes from the typical quasi-triangular well shape in the vicinity where the 2DEG ultimately forms into a pair of quasi-triangular wells due to the conduction band offsets at both the $AlN/Al_{0.1}Ga_{0.9}N$ and $Al_{0.1}Ga_{0.9}N/GaN$ interfaces. This phenomenon gives rise to the second and most important point: despite the same total charge in the channel (1×10^{13} cm^{-2}), the electrons have been effectively spread out in the camelback channel and resulted in a reduced peak 3D electron density as compared to the 2DEG in the standard structure. This is important as the 3D electron density is believed to be the parameter responsible for hot-phonon interaction with plasmons; once the 3D density is reduced, the hot-electron–hot-phonon system is closer to the plasmon–LO-phonon crossover and exhibits shorter hot-phonon lifetimes.

In light of the fact that hot electrons within a GaN-based HFET channel are known to reach thousands of K under bias, Schrödinger–Poisson equations have been again solved at elevated electron temperatures for the camelback structure. The results are displayed in Fig. 3. One can see the expected spreading of the electron distribution with the temperature, resulting from the increased occupation of upper subbands by hot electrons in the coupled wells of the composite channel. Due to this, the camelback shape of the profile for which the structure is named begins to emerge; it appears as though the original 2DEG is splitting, with the resultant 2DEG having lower overall 3D density but in fact containing the same total charge (1×10^{13} cm^{-2}).

III. EXPERIMENT

A camelback HFET structure was grown on a sapphire substrate by metalorganic chemical vapor deposition (MOCVD). The structure consisted of a low temperature

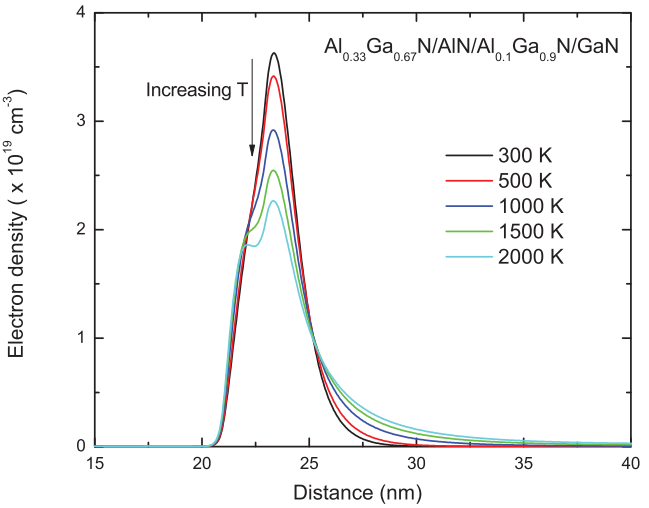

FIG. 3. (Color online) Calculated electron 3D density as a function of electron temperature for the camelback structure. In each curve, the integrated density of electrons equals 1×10^{13} cm^{-2}. The dual peaked 2DEG (camelback) is pronounced at elevated temperatures.

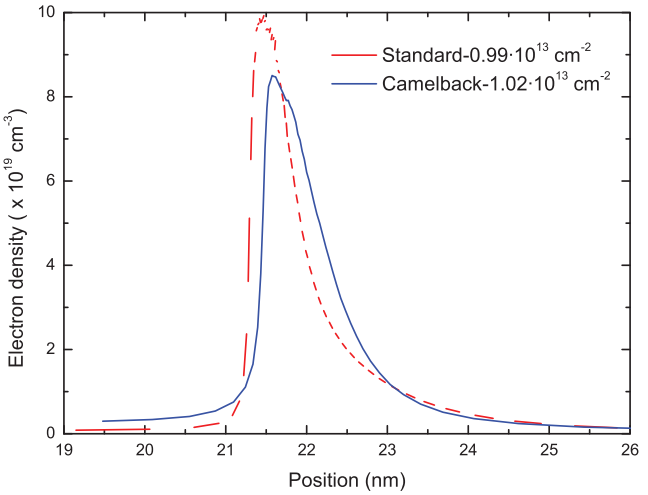

FIG. 4. (Color online) Electron 3D density profiles measured by capacitance–voltage technique for the camelback structure (solid) as well as the standard structure (dashed).

AlN buffer layer followed by 2 microns of GaN, a 2 nm $Al_{0.1}Ga_{0.9}N$ camelback layer, a 1 nm AlN spacer layer, and a 20 nm $Al_{0.33}Ga_{0.67}N$ barrier layer. Trimethyl-gallium, trimethyl-aluminum, and ammonia were used as the Ga, Al, and N sources, respectively. Ni/Au and Ti/Al/Ni/Au metal stacks were deposited to fabricate Schottky diodes as well as Ohmic contacts for transmission line method (TLM) patterns, respectively. The diodes were used for capacitance–voltage measurements to assess the total charge density of the mobile electrons (2DEG density) and the electron 3D density profile. The TLM patterns were used for microwave noise analysis to assess the hot-phonon lifetime. In these measurements, the noise temperature of the structure is measured as a function of applied power during voltage pulsing.[13] The data are then compared with a standard AlGaN/AlN/GaN structure[7] without the composite channel to assess the effect of the camelback profile on the electron distribution as well as the hot-phonon lifetime.

IV. EXPERIMENTAL RESULTS AND DISCUSSION

From the simulations, it is apparent that the camelback approach is effective in reducing the peak 3D density of a 2DEG with a fixed total charge (1×10^{13} cm^{-2} in this case). To access this information experimentally, capacitance–voltage (C–V) measurements can be employed to plot electron 3D density profiles as a function of the depth into the structure. Subsequently, the total 2DEG density can be estimated by integrating these 3D densities obtained from the C–V measurement. Shown in Fig. 4 are the experimental density profiles for the camelback structure as well as a standard AlGaN/AlN/GaN structure for comparison. The standard structure was selected due to its similarity to the camelback structure in terms of the total 2DEG density; through integration, the standard and camelback structures exhibit total 2DEG densities of 0.99×10^{13} and 1.02×10^{13} cm^{-2}. Despite the similarity in 2DEG densities, the half-width of the 2DEG in the camelback structure ($\sim$0.8 nm) is larger than that of the standard structure ($\sim$0.6 nm), as anticipated from the simulation. Thus, the camelback structure with a lower 3D electron density than the standard structure should exhibit a shorter hot-phonon lifetime than the standard structure.

To obtain the hot-phonon lifetime in a 2DEG, the microwave noise technique is employed.[13] In this technique, voltage pulses are applied to a pair of Ohmic contacts, and the noise power emitted from the channel at 10 GHz is compared to that of a blackbody radiator kept at a known temperature. Since the sample is not a true blackbody, additional measurements are performed for estimation of the sample reflection coefficient at each bias and power loss in the input microwave circuit. At 10 GHz, low frequency sources of noise such as 1/f noise and noise associated with trapping can be neglected—the microwave noise can be attributed to electron scattering.

Figure 5 shows the measured excess noise temperature (temperature in excess of room temperature) as a function of the power supplied to an average electron present in the camelback channel. The circles represent the temperature estimated for voltage pulse duration of 2.7 μs while the squares and triangles stand for 100 and 50 ns pulse durations, respectively. The equivalent results for both pulse widths at moderate pulsed power in the camelback structure indicate negligible self-heating. Additionally, no evidence of an additional source of noise arising from electronic transitions from "shared" states (between the $Al_{0.1}Ga_{0.9}N$ and GaN) to "confined" states and back to the "shared" states[17] could be observed, validating the technique's use in the camelback structure.

Consider power dissipated by hot phonons. Once a constant hot-phonon lifetime τ_{LO} is assumed, the dissipated power is proportional to the excess occupancy of the hot phonon modes, $P_d = A\left(N^*_{LO} - N_0\right)$ where N^*_{LO} is the equivalent occupancy of the LO-phonon states (occupied by the hot phonons emitted by the hot electrons) and $A = \hbar\omega_{LO}/\tau_{LO}$. For the dominant electron–LO-phonon interaction and strong hot-phonon effects, the noise temperature, T_{noise},

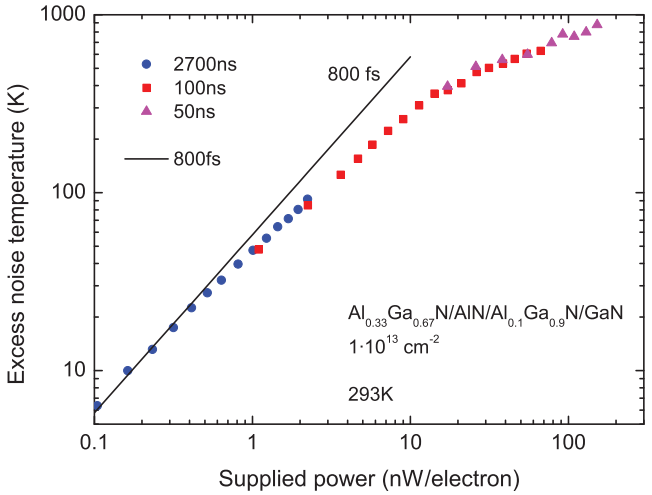

FIG. 5. (Color online) Measured excess noise temperature, equal to the electron temperature, for the camelback structure as a function of applied power. Circles represent pulse widths of 2.7μs, squares stand for 100 ns, and triangles represent 50 ns.

approximately equals the hot-electron temperature, T_e, while the latter almost equals the equivalent hot-phonon temperature T_{LO}.[18] Thus, the equivalent occupancy N^*_{LO} can be estimated after the Bose–Einstein formula if $T^*_{LO} \approx T_e$ is assumed (the validity of the assumption has been checked previously[17,19,20]). This leads to

$$P_d = A\left\{\left[\exp\left(\hbar\omega_{LO}\Big/k_B T_e\right) - 1\right]^{-1} - \left[\exp\left(\hbar\omega_{LO}\Big/k_B T_0\right) - 1\right]^{-1}\right\}. \quad (2)$$

Equation (2) is a modified Arrhenius law. It states that an electron can take part in power dissipation if its energy exceeds the LO phonon energy. Solid lines in Fig. 6 illustrate Eq. (2) when constant values of 200 and 300 fs are used for the hot-phonon lifetime. Note that the experimental data (symbols) remain in between the curves in the temperature range below ~600 K ($\sim 1.6\times10^{-3}$ K^{-1}). In this range, the power dissipation is mainly controlled by the electron interaction with the hot LO phonons treated in terms of constant hot-phonon lifetime.However, the hot-phonon lifetime seems to depend on the applied power at high temperatures, and a dynamic lifetime can be introduced,

$$\tau^*_{LO} = \hbar\omega_{LO} dN^*_{LO}\Big/dP_d. \quad (3)$$

Figure 7 shows the results for the dynamic hot-phonon lifetime as a function of the supplied power for the camelback structure (squares). At low–moderate supplied pulsed powers (<10 nW/e), the hot-phonon lifetime for the camelback channel structure is nearly constant and approximately equals ~270 fs.

Electron energy dissipation is often treated in terms of hot-electron energy relaxation time. Under a fixed value of the relaxation time, τ_{energy}, the electron temperature increases linearly with applied power, P_A, in accordance with $k_B(T_e - T_0) = P_A\tau_{energy}$. The energy relaxation time at zero applied power is close to 800 fs (solid line in Fig. 5). This value exceeds the low-power value of the hot-phonon lifetime of 270 fs estimated in the power range below 10 nW/electron where the lifetime is almost independent of the power (Fig. 7, squares). The energy relaxation time appears to depend on the applied power as well. In this case, a dynamic energy relaxation time can be introduced, $\tau^*_{energy} = k_B(dT_e/dP_A)$, which is plotted in Fig. 7 (circles). The value of the energy relaxation time appears to be ~700–800 fs under low (<1 nW/electron) supplied power, but decreases with increasing supplied power, and eventually τ^*_{energy} merges with the dynamic hot-phonon relaxation time τ^*_{LO} at a power of ~10 nW/electron. This happens at a hot-electron temperature exceeding ~600 K (Fig. 5) when many of the electrons have sufficient energy to emit LO phonons.

Figure 8 compares the hot-phonon lifetime for two camelback channels (triangles and stars) and a reference channel (squares) when the channels have the same 2DEG density

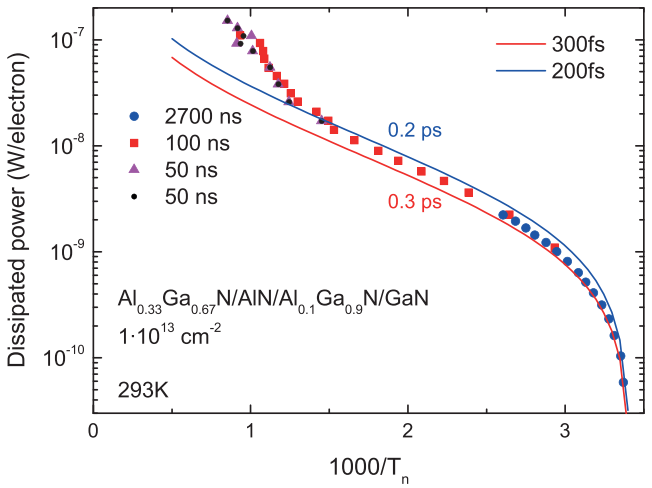

FIG. 6. (Color online) Arrhenius plot of experimental dissipated power against inverted noise temperature for the camelback structure (symbols) along with Eq. (2) that assumes constant hot-phonon lifetimes of 200 fs and 300 fs (solid lines, blue and red, respectively).

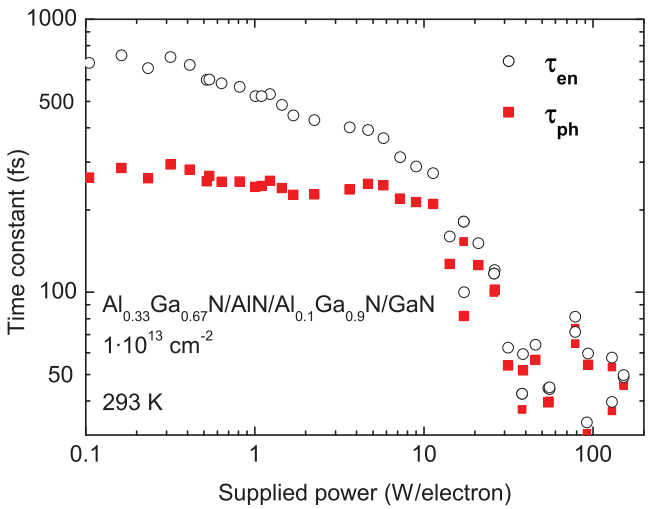

FIG. 7. (Color online) Dynamic energy relaxation time (circles) and dynamic hot-phonon lifetime (squares) as functions of the supplied power for the camelback structure.

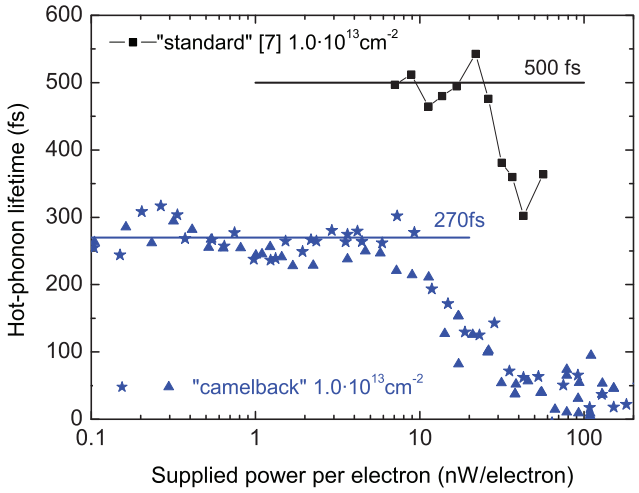

FIG. 8. (Color online) Hot-phonon lifetime measured by the microwave noise technique for the standard channel (squares, Ref. 7) as well as camelback channels (stars, triangles) with equal 2DEG densities (1×10^{13} cm^{-2}).

(1×10^{13} cm^{-2}). Two important phenomena are noted. First, the low-power value of the hot-phonon lifetime is reduced from ~500 fs in the standard channel to ~270 fs in the camelback channel. Next, both the camelback channel as well as the standard channel exhibit a rapid decline in the hot-phonon lifetime at high power levels, but several times higher power is needed for the decline to take place in the standard channel. The properties of the camelback channel are reproducible (stars and triangles).

Let us discuss the results. Despite nearly identical 2DEG density (1×10^{13} cm^{-2}), the channels have different electron density profiles (Fig. 4). Since the electron 3D density is lower in the camelback channel, and the plasma frequency is closer to that of the uncoupled LO phonons. In accordance with the plasmon-assisted decay of hot phonons, the camelback channel demonstrates the reduced hot-phonon lifetime at low power, Fig. 8 (stars, triangles). Having said this, one cannot rule out the possibility that the phonon lifetime in the camelback channel is shorter at low power simply as a result of the addition of the AlGaN alloy, as theory predicts[21] and experiment has shown[22,23] the phonon lifetime to be shorter in AlN as compared to GaN. Further experiments utilizing camelback channels with different compositions and 2DEG densities will elucidate this. Nevertheless, under electron heating, the power-assisted spreading of the electron density profile takes place and causes the 3D density to approach the plasmon–LO-phonon crossover value.[14] This happens in both the camelback channel as well as the standard structure, and the associated rapid decline in hot-phonon lifetime is observed at elevated power levels. However, the camelback structure exhibits the rapid decline in hot-phonon lifetime at a lower supplied power than the standard structure, despite having equal total 2DEG densities. This point indicates that the short lifetimes observed in the camelback channel are associated with LO-phonon–plasmon interactions and not merely due to an intrinsically shorter lifetime in the camelback channel.

The decline in hot-phonon lifetime with supplied power is attributed to a significant spreading of the electron density profile when the electrons begin to fill the second subband of the quantum well at the hot-electron temperatures associated with these supplied powers (above 600 K according to Figs. 5 and 6). Such a phenomenon is evidenced from the simulation in Fig. 3 which shows the electron profile as a function of the electron temperature. Significant profile spreading takes place between temperatures from 500 to 1000 K according to Fig. 3. Higher electron temperatures and consequently higher applied power are required to fill the upper subbands in the standard structure,[14] and therefore the rapid decline of the hot-phonon lifetime is not achieved until several times higher power is applied to the standard structure. The camelback structure has been successfully designed to reduce the 3D density of electrons in a HFET channel at zero bias and demonstrates a shorter low-power value of the hot-phonon lifetime at a given 2DEG density. Moreover, it also exhibits a lower threshold for the rapid decline of the hot-phonon lifetime caused by the power-assisted spreading of the 2DEG profile.

V. CONCLUSIONS

The effect of hot phonons on HFET devices cannot be overstated in that hot phonons suppress electron velocity, can stimulate a formidable source of degradation in HFET devices, and essentially frustrate attempts to increase the 2DEG density in HFET channels in the quest to achieve higher frequencies and higher output powers. For this reason, the ability to tune the hot phonon lifetime technologically while maintaining the total 2DEG electron density is an important finding and crucial for advanced device design. We know that the hot-phonon effect can only be mitigated in 2DEG channels if the hot-phonon lifetime can be reduced. This may be achieved technologically by carefully designing the heterostructure such that the 2DEG density is near the plasmon–LO-phonon crossover value under operating conditions.

The $Al_{0.1}Ga_{0.9}N$ layer for a camelback channel described in this work could alternatively be replaced with the InGaN layer sandwiched between two GaN layers in the channel, or a number of other combinations of InGaN and AlGaN-based composite channels. In this sense one can envision a carefully tailored heterostructure in which the total number of electrons in the channel is high but the 2DEG is spread out and a lower volume density of electrons is attained. In this way, relatively high powers can be achieved while simultaneously reducing the hot-phonon lifetime and its corresponding deleterious effects.

ACKNOWLEDGMENTS

This work is supported by Grants Nos. FA8655-09-1-3103 and FA9550-04-1-04-14 from the U.S. Air Force Office of Scientific Research under the direction of Dr. Kitt Reinhardt. One of us (E. S.) is grateful for the postdoctoral fellowship funded by the European Union Structural Funds project "Postdoctoral Fellowship Implementation in Lithuania."

[1]H. Morkoç, *Handbook of Nitride Semiconductors and Devices* (John Wiley and Sons, New York, 2008).
[2]M. Rosker, C. Bozada, H. Dietrich, A. Hung, D. Via, S. Binari, E. Vivieros, E. Cohen, and J. Hodiak, paper presented at the CS MANTECH Conference, Tampa FL, May 2009.
[3]M. Higashiwaki, T. Mimura, and T. Matsui, IEICE Trans. Electron. **E91-C**, 984 (2008).
[4]M. Higashiwaki, T. Mimura, and T. Matsui, Appl. Phys. Express **1**, 021103 (2008).
[5]K. Tsen, R. P. Joshi, D. K. Ferry, A. Botchkarev, B. Sverdlov, A. Salvador, and H. Morkoç, Appl. Phys. Lett. **68**, 2990 (1996).
[6]B. K. Ridley, W. J. Schaff, and L. F. Eastman, J. Appl. Phys. **96**, 1499 (2004).
[7]A. Matulionis, Phys. Stat. Solidi A. **203**, 2313 (2006).
[8]J. H. Leach, C. Y. Zhu, M. Wu, X. Ni, X. Li, J. Xie, Ü. Özgür, H. Morkoç, J. Liberis, E. Šermukšnis, A. Matulionis T. Paskova, E. Preble, and K. R. Evans, Appl. Phys. Lett. **96**, 133505 (2010).
[9]M. Ramonas and A. Matulionis, Semicond. Sci. Technol. **19**, S424 (2004).
[10]J. H. Leach, C. Y. Zhu, M. Wu, X. Ni, X. Li, Ü. Özgür, H. Morkoç, J. Liberis, E. Šermukšnis, A. Matulionis, H. Cheng, and C. Kurdak, Appl. Phys. Lett. **95**, 223504 (2009).
[11]K. T. Tsen, J. G. Kiang, D. K. Ferry, and H. Morkoç, Appl. Phys. Lett. **89**, 112111 (2006).
[12]A. Dyson and B. K. Ridley, J. Appl. Phys. **103**, 114507 (2008).
[13]A. Matulionis, J. Liberis, I. Matulionienë, M. Ramonas, L. F. Eastman, J. R. Shealy, V. Tilak, and A. Vertiatchikh, Phys. Rev. B **68**, 035338 (2003).
[14]A. Matulionis, J. Liberis, I. Matulionienë, M. Ramonas, and E. Ðermukõnis, Proc. IEEE **98**, 1118 (2010).
[15]Z. Wang, K. Reimann, M. Woerner, T. Elsaesser, D. Hofstetter, J. Hwang, W. J. Schaff, and L. F. Eastman, Phys. Rev. Lett. **94**, 037403 (2005).
[16]J. H. Leach, M. Wu, H. Morkoç, M. Ramonas, and A. Matulionis, Proc SPIE **7939**, 79391P (2011).
[17]A. Matulionis, J. Liberis, L. Ardaravièius, M. Ramonas, T. Zubkutë, I. Matulionienë, L. F. Eastman, J. R. Shealy, J. Smart, D. Pavlidis, and S. Hubbard, Phys. Stat. Solidi B **234**, 826 (2002).
[18]J. Liberis, I. Matulionienë, A. Matulionis, M. Ramonas, and L. F. Eastman, in *Advanced Semiconductor Materials and Devices Research: III-Nitrides and SiC*, edited by Ho-Young Cha (Transworld Research Network, Kerala, 2009), pp. 203–242.
[19]A. Matulionis, J. Liberis, M. Ramonas, I. Matulionienë, L. F. Eastman, A. Vertiatchikh, X. Chen, and Y. J. Sun, Phys. Stat. Solidi C **2**, 2585 (2005).
[20]A. Matulionis, J. Phys.: Condens. Matter **21**, 174203 (2009).
[21]Srivistava, Phys. Rev. B **77**, 155205 (2008).
[22]K. T. Tsen, D. K. Ferry, A. Botchkarev, B. Sverdlov, A. Salvador, and H. Morkoç, Appl. Phys. Lett. **72**, 2132 (1998).
[23]M. Kuball, J. M. Hayes, Y. Shi, and J. H. Edgar, Appl. Phys. Lett. **77**, 1958 (2000).